Voltage-Dependent Behavior of a "Ball-and-Chain" Gramicidin Channel

G. Andrew Woolley, Valentin Zunic, John Karanicolas, Anna S. I. Jaikaran, and Andrei V. Starostin

Department of Chemistry, University of Toronto, Toronto, Ontario M5S 3H6, Canada

ABSTRACT   The channel-forming properties of two analogs of gramicidin, gramicidin-ethylenediamine (gram-EDA), and gramicidin-N,N-dimethylethylenediamine (gram-DMEDA) were studied in planar lipid bilayers, using protons as the permeant ion. These peptides have positively charged amino groups tethered to their C-terminal ends via a linker containing a carbamate group. Gram-DMEDA has two extra methyl groups attached to the terminal amino group, making it a bulkier derivative. The carbamate groups undergo thermal *cis-trans* isomerization on the 10–100-ms time scale. The conductance behavior of gram-EDA is found to be markedly voltage dependent, whereas the behavior of gram-DMEDA is not. In addition, voltage affects the *cis-trans* ratios of the carbamate groups of gram-EDA, but not those of gram-DMEDA. A model is proposed to account for these observations, in which voltage can promote the binding of the terminal amino group of gram-EDA to the pore in a "ball-and-chain" fashion. The bulkiness of the gram-DMEDA derivative prevents this binding.

INTRODUCTION

The gramicidin ion channel is sufficiently well characterized that rational approaches to the engineering of novel channel behaviors are possible (Koeppe and Andersen, 1996). We have been interested in designing "gates" for gramicidin so that channel activity can be controlled by external stimuli (e.g., light (Lien et al., 1996; Stankovic et al., 1991; Sukhanov et al., 1993) or a voltage pulse (Oiki et al., 1995; Woolley et al., 1995)). Such designed channels could be useful as tools for studying cellular excitability. Several studies have shown that charged groups at the C-terminal ends of gramicidin can have large effects on channel conductance (Apell et al., 1977, 1979; Bamberg et al., 1978; Jin, 1992; Reinhardt et al., 1986; Roeske et al., 1989). Controlling the position of such groups might provide a means of gating the channel.

We recently described the synthesis and characterization of gramicidin derivatives bearing positively charged amino groups linked via carbamate bonds to the C-terminal ends of the channel (Jaikaran and Woolley, 1995; Woolley et al., 1995). Thermal *cis-trans* isomerization of the carbamate linkages was found to have pronounced effects on ion flux. Four different conducting states could be identified in single-channel records of gramicidin ethylenediamine (gram-EDA) corresponding to the four conformational states of the two carbamate bonds, one at each end of the channel. In addition, the conductances corresponding to conformers with *cis*-carbamate bonds were found to be distinctly voltage dependent (Woolley et al., 1996) .

We were motivated to undertake a detailed study of the origins of these conductance changes because we felt that this would help guide efforts to design useful gated gram-

icidin analogs. In addition, we felt that studies with this well-defined model system might lead to insights into the behavior of other, more complex, tethered gating particles that occur in natural protein ion channels (the "ball-and-chain" paradigm; Hille, 1992).

Previous studies of gramicidin analogs bearing negative charges at the channel entrances (and exits) have characterized in detail the effects of such charges on the channel conductance. Taurine-gramicidin (Roeske et al., 1989), with a C-terminal sulfate, and desethanolamine gramicidin (Reinhardt et al., 1986) with a C-terminal carboxylate bear single negative charges; gramicidin pyromellitate (Apell et al., 1977) bears three negative charges at neutral pH (Cifu et al., 1992). In each of these cases, the negative charges were found to increase cation conductance at low to moderate ion concentrations. At high ion concentrations (> 1 M), the observed conductance was similar to or less than that of unmodified gramicidin. Single-channel current-voltage (I-V) measurements of heterodimer channels (in which only one monomer is modified) demonstrated that the effect of the negative charge was more pronounced when it was at the channel entrance, rather than the exit, for both the taurine and the pyromellitate derivatives. This behavior can be understood in terms of an electrostatic model in which the negative charge(s) concentrates cations at the channel entrance and thus facilitates ion entry into the channel. As the bulk solution concentration of ions increases, the effect of the negative charge on channel conductance diminishes and steric effects dominate (Cifu et al., 1992). Smaller conductance increases resulting from a negative charge at the channel exit have been suggested to result from a long-range electrostatic effect on ion translocation (Jin, 1992; Cifu et al., 1992; MacKinnon et al., 1989).

For the purposes of gating gramicidin, a controlled decrease, rather than increase, in gramicidin conductance is required. Bamberg et al. published a short report of the properties of a positively charged gramicidin analog, *p-N*-trimethylammonium-benzoyl gramicidin, in which they showed that the positive charge had the expected opposite

effect, i.e., conductance was diminished 1.6-fold in 0.2 M CsCl (Bamberg et al., 1978). Although a comprehensive analysis was not reported, it appears that, in this case too, the effect on the conductance depended on whether the charge was at the channel entrance or exit.

In attempting to understand the conductance properties of these charged gramicidin derivatives, it is important to consider whether the voltage might alter the average location of the charge relative to the pore (Jin, 1992). Whether this occurs will depend on the conformational flexibility of the chemical modification. The pyromellityl and the p-N-trimethylammonium-benzoyl groups are bulky, relatively rigid structures, and the taurine derivative has the negative charge only a short distance from the polypeptide backbone. Thus only limited conformational changes are possible for these groups, and the applied voltage is unlikely to greatly alter the average positions of the charges.

In contrast, the C-terminal arm of gram-EDA is relatively flexible. In addition to the carbamate bond, seven rotatable single bonds connect the charged amino group to the peptide backbone. Molecular models show that it is possible for the C-terminal arm of gram-EDA to adopt conformations that occlude the pore completely. The arm resembles somewhat a "tethered" ammonium ion; ammonium ions and methylammonium ions are known to permeate the gramicidin channel (Andersen, 1983; Eisenman et al., 1977; Myers and Haydon, 1972; Seoh and Busath, 1993). If the charged amino group on the arm were to actually enter the channel or, at least, were to sense the applied transmembrane potential, then the conformational behavior of the arm would be voltage dependent.

The present work describes a study of the properties of the gram-EDA system as a function of voltage with protons as the permeant ions. We find that the applied potential affects cis-trans ratios of the carbamate bonds in the C-terminal arms and so ipso facto affects the conformation of the arms. This voltage effect on carbamate conformation can be understood in terms of a simple model in which the tethered ammonium group can interact directly with the pore. This interaction is stabilized by a voltage of the correct sign and is stabilized more for a tether with a cis-carbamate bond than for one with a trans bond.

If it is assumed that interaction of the tether occludes the pore, then the model predicts that the conductance properties of gram-EDA channels should also be voltage dependent. Single-channel I-V relationships for each of the four conformational states of the gram-EDA channel are consistent with such a model. Also consistent is the behavior of a bulkier analog, gramicidin-N-dimethyl-ethylenediamine (gram-DMEDA). This derivative shows almost no voltage dependence of the cis-trans carbamate ratio, or of single-channel conductance. These observations can be explained if the N-methyl groups prevent, via steric effects, interaction of the tether with the pore and thereby prevent the charge from sensing the applied voltage.

MATERIALS AND METHODS

Gramicidin-ethylenediamine (gram-EDA) and gramicidin-N,N-dimethyl-ethylenediamine (gram-DMEDA) were prepared and purified as described previously (Woolley et al., 1995). Diphytanoylphosphatidylcholine was obtained from Avanti Polar Lipids (Alabaster, AL) and dissolved in decane (Aldrich) at a concentration of 50 mg/ml. Lipid bilayers were formed over the opening of a pipette tip as described by Busath and Szabo (1988). Currents through lipid bilayers containing the gramicidin derivatives were recorded and controlled with an Axopatch 1D patch-clamp amplifier (Axon Instruments). The recordings were obtained at 23°C (± 2°C) and filtered at 200 Hz except where noted. Silver/silver chloride electrodes were connected to the solutions bathing the bilayer via agarose/KCl salt bridges. Current recordings were stored and analyzed with Synapse software (Synergistic Research Systems). Amplitude histograms were constructed and analyzed with Igor Pro software (Wavemetrics). Because relative, not absolute, areas of the peaks in the amplitude histograms were of interest, the following procedure for calculating areas was used. When a single channel was open (i.e., a conducting gramicidin dimer was present), current values were binned until the relative areas of histogram peaks corresponding to the different conducting states became constant (± 10%). Typically this corresponded to 10-20 s of dimer open time. Areas were calculated by fitting histogram peaks with Gaussian curves and integrating the area between inflection points in the curves. Areas were normalized so that the sum of the areas was one.

Gradients of H$^+$ across the membrane were established as follows. First, channels were obtained with 0.1 M HCl solutions on both sides of the membrane. Then the hole separating the aqueous compartments was plugged with lipid, and sufficient concentrated Tris (tris[hydroxymethyl]aminomethane) base solution (2 M) was added to one compartment only to bring the H$^+$ concentration to 0.01 M. H$^+$ ion concentrations were measured with a pH meter that had been calibrated for this pH range. After formation of the gradient, a bilayer was reformed without breaking the seal, and single-channel recording continued. The zero-current potential did not change during the course of the experiment, as was confirmed at the end of the experiment when the bilayer was broken.

Simultaneous fitting of Eqs. 5 and 8-11 to experimental data was performed interactively with the Igor Pro data analysis package.

RESULTS

Fig. 1 shows single-channel records of gramicidin-ethylenediamine (gram-EDA) channels in diphytanoyl-PC/de-
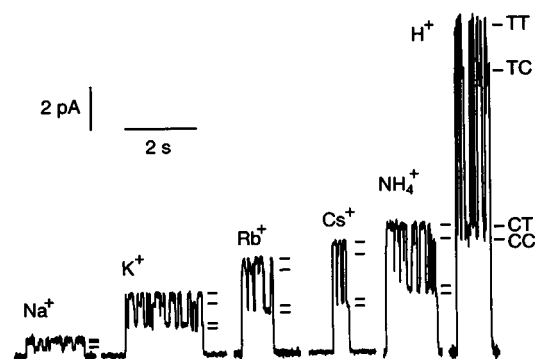

FIGURE 1   Single-channel currents of gram-EDA in various salt solutions at 150 mV applied potential. All solutions are 1 M of the indicated ion (with Cl$^-$ as the counterion), 5 mM N,N-bis(2-hydroxyethyl)-2-aminoethanesulfonic acid (pH 6.3), except for HCl, where the concentration was 0.1 M (with no added buffer). Channels open upward, and four conductance states (indicated by the bars) are observed above the baseline in each case (except Na$^+$, for which the levels are poorly resolved).

TABLE 1 Measured conductances of gram-EDA in different salt solutions

Salt solution	Level 1 (pS)	Level 2 (pS)	Level 3 (pS)	Level 4 (pS)
1 M NaCl	4.8	3.7	2.3	ND
1 M KCl	16.8	14.3	8.5	7.3
1 M RbCl	26	22.6	12	ND
1 M CsCl	30.8	28.1	13.9	12.6
1 M NH₄Cl	35	30.1	18.1	15.6
0.1 M HCl	87.6	74.4	34.8	31

Applied voltage 150 mV; diphytanoyl-PC/decane membranes; 23°C. ND, Not determined.

cane bilayers recorded for a series of different symmetrical salt solutions with an applied voltage of 150 mV (Table 1). Qualitatively similar conductance behavior is seen in all cases, i.e., four different conductance states in addition to the baseline (closed channel). In order of decreasing conductance, these were found to correspond to *trans-trans* (TT), *trans*(entrance)-*cis*(exit) (TC), *cis*(entrance)-*trans*(exit) (CT), and *cis-cis* (CC) conformations of the carbamate groups at the channel ends (Woolley et al., 1995). Structural models of these states are shown in Fig. 2, where the conformations of the carbamates are highlighted.
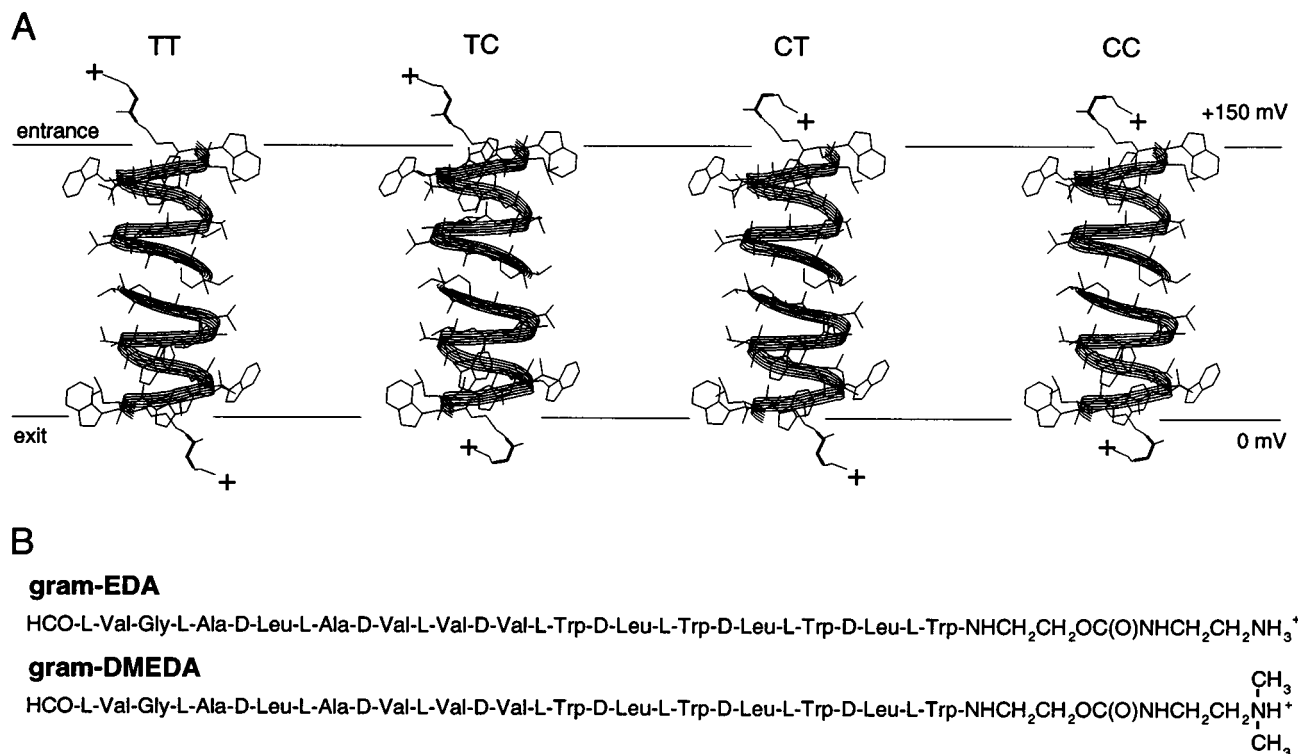
All of the currents, including that of the TT state, are significantly reduced (at least 30%) compared to unmodified gramicidin channels under the same conditions

(Andersen, 1983; Myers and Haydon, 1972). The variation of current magnitude with cation-type parallels the order seen with the native peptide (Andersen, 1983; Myers and Haydon, 1972). Because the different conductance states were particularly well defined in HCl solutions, these were employed for characterizing the voltage-dependent behavior of the channels.

Voltage-dependent conductance behavior of gram-EDA

Fig. 3 shows the effect of voltage on the appearance of single-channel currents of gram-EDA in 0.1 M HCl. Whereas the largest conductance state (TT) has a nearly linear *I-V* relationship (Fig. 3 *B*), the *cis*-entrance, *trans*-exit (CT) state, for example, has an *I-V* relationship that curves toward the voltage axis with positive voltages. The *trans*-entrance/*cis*-exit (TC) conformer has an *I-V* relationship that is symmetrical with the CT state about the origin. This behavior is expected, because the gram-EDA channel is a symmetrical dimer; when the voltage is reversed, a *cis*-carbamate at the entrance becomes a *cis* at the exit. Finally, the *cis-cis* (CC) state also has a nonlinear but symmetrical *I-V* relationship.

When these data are plotted as chord conductance versus voltage (Fig. 4), the voltage dependence of the conductance

A

TT   TC   CT   CC

entrance   +150 mV

exit   0 mV

B

gram-EDA

HCO-L-Val-Gly-L-Ala-D-Leu-L-Ala-D-Val-L-Val-D-Val-L-Trp-D-Leu-L-Trp-D-Leu-L-Trp-D-Leu-L-Trp-NHCH₂CH₂OC(O)NHCH₂CH₂NH₃⁺

gram-DMEDA

HCO-L-Val-Gly-L-Ala-D-Leu-L-Ala-D-Val-L-Val-D-Val-L-Trp-D-Leu-L-Trp-D-Leu-L-Trp-D-Leu-L-Trp-NHCH₂CH₂OC(O)NHCH₂CH₂NH⁺

$$\begin{array}{c} CH_3 \\ | \\ NHCH_2CH_2NH^+ \\ | \\ CH_3 \end{array}$$

FIGURE 2 (*A*) Structural models of each of the four conformational states of gram-EDA. They differ in the conformation of the carbamate bond in the arm (*bold lines*). From left to right they are: TT (*trans* entrance–*trans* exit), TC (*trans* entrance–*cis* exit), CT (*cis* entrance–*trans* exit), and CC (*cis* entrance–*cis* exit). The models are based on the structure of Ketchem et al. (1993). Single bond rotations make the arms flexible, so that only one of many possible conformations is shown in each case. (*B*) Primary structures of gram-EDA and gram-DMEDA.
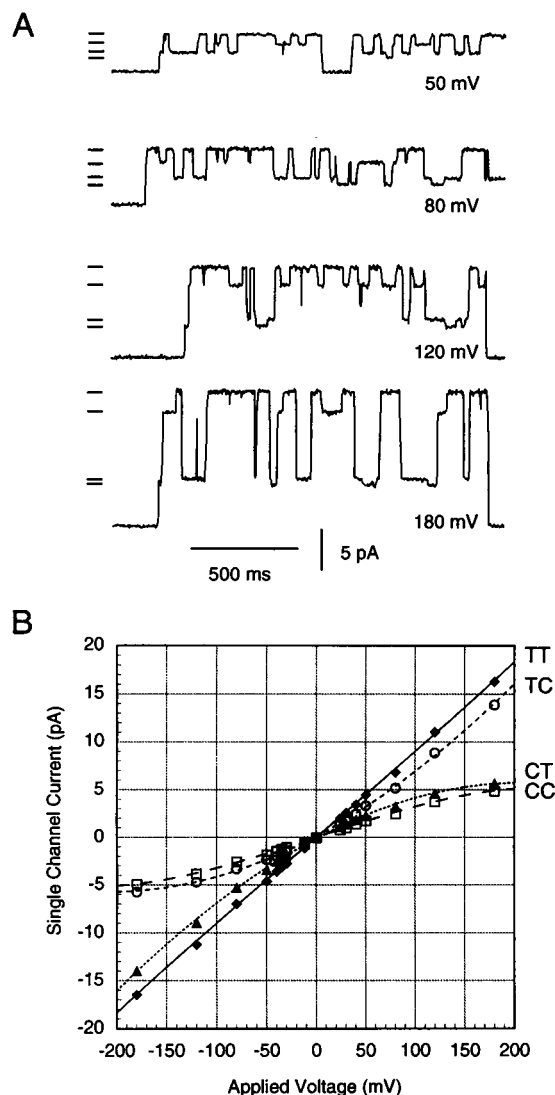
FIGURE 4   (A) Single-channel (chord) conductance-voltage relationships for each state of gram-EDA: ◆, TT state; ○, TC state; ▲, CT state; □, CC state. Fitted curves are calculated using equations 8–11 in the text. (B) Comparison of gram-EDA single-channel conductances at 50 mV and 180 mV (indicated by *dashed lines* in A). Channels open upward; the lowest level is the closed channel, and conductance states are indicated by the bars. Note that the two middle conductance states (TC and CT) are particularly affected by voltage.

FIGURE 3   (A) Single-channel currents of gram-EDA in 0.1 M HCl at different voltages. Channels open upward from the baseline. The sign of the voltage refers to the channel entrance (see Fig. 2). Four different conductance states indicated by the bars are observed at each voltage. (B) Single-channel current-voltage relationships for each conductance state of gram-EDA: ◆, TT state; ○, TC state; ▲, CT state; □, CC state.

of the CT and TC states is evident. Fig. 4 *B* shows clearly how an increased voltage causes the conductances of the CT and TC states to diverge.

Single-channel currents in the presence of a pH gradient

We examined whether the channel conductance behavior depended on the source of the driving force for proton movement. Fig. 5 shows single-channel *I-V* relationships in the presence and absence of a pH gradient.

This pH gradient provides a driving force for proton flux of ~35 mV, based on the observed reversal potential. When the applied voltage is zero, this results in a current of 2.5 pA
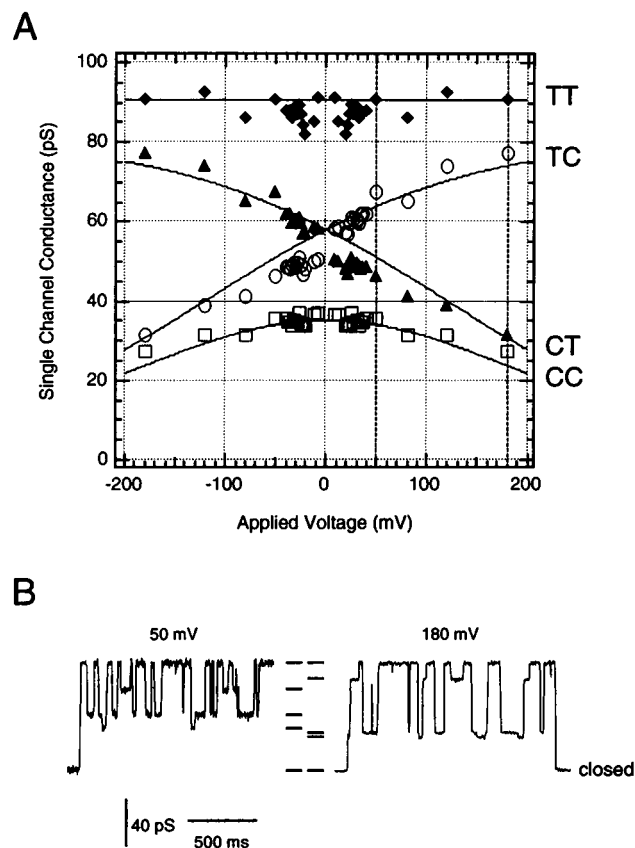
for the *trans-trans* (TT) state. When the same driving force (i.e., 35 mV) is provided by an applied voltage in the absence of a pH gradient, the current observed for the TT state is the same (Fig. 5, *B* and *C*). Different behavior is observed for the CT and TC states, however. In the absence of an applied voltage, the CT and TC states have nearly identical conductances. When a voltage is applied, the conductances of these two states diverge; the conductance of the CT state is less than at zero applied voltage, whereas that of the TC state is greater. The applied voltage is therefore doing something more than simply providing a driving force for protons.
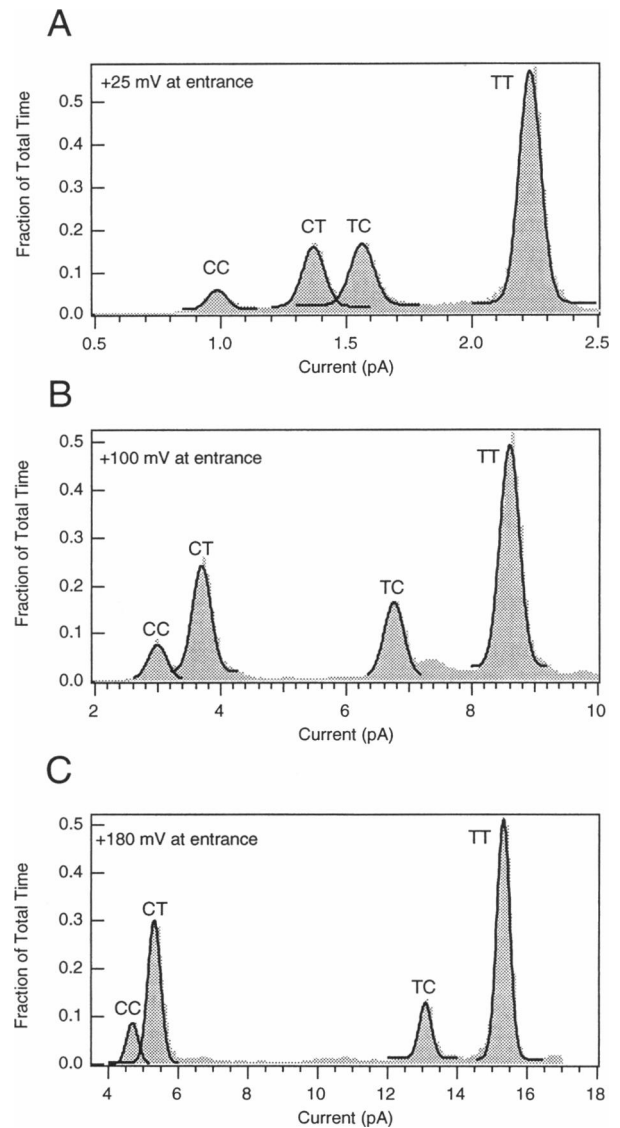
Voltage dependence of *cis-trans* carbamate ratios in gram-EDA

A direct indication of whether the voltage is affecting the conformation of the "gate" can be obtained by measuring the fraction of *cis* and *trans* carbamate isomers at different applied potentials. All-point histograms representing the
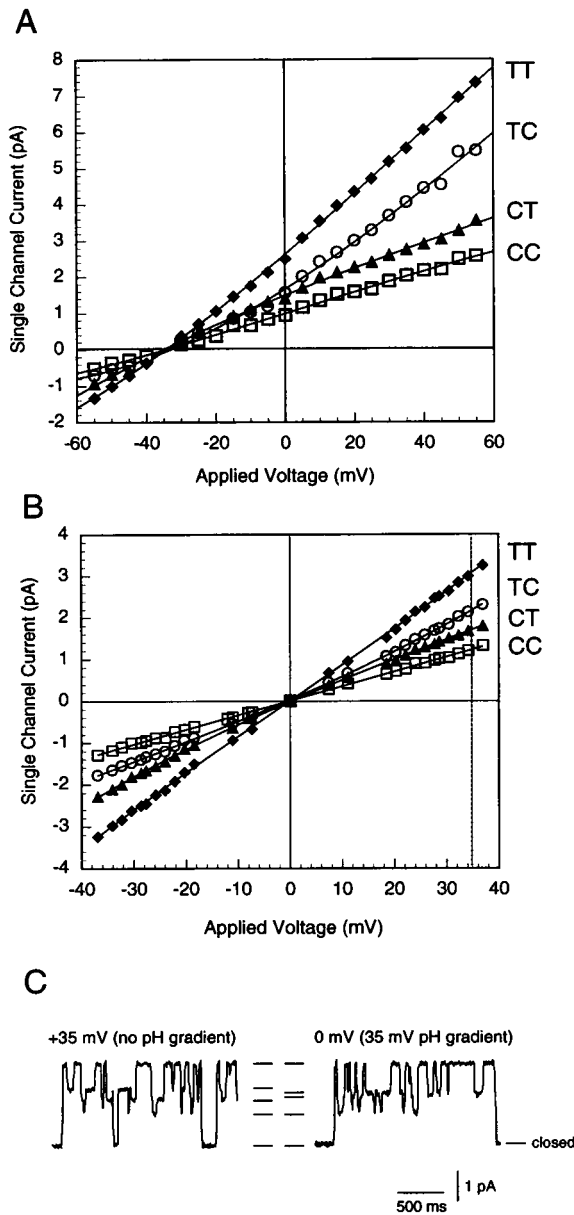
FIGURE 5 Single-channel current-voltage relationships for gram-EDA in the presence (A) and absence (B) of a pH gradient. ♦, TT state; ○, TC state; ▲, CT state; □, CC state. (C) Comparison of gram-EDA single-channel currents, where the magnitude of the driving force for proton movement is the same, but the source of the driving force is either an applied voltage (*left*) or a pH gradient (*right*). Note that the conductance of the TC and CT states is sensitive to the source of the driving force.

FIGURE 6 All-point histograms of time spent by gram-EDA in each conducting state at 25 mV (A), 100 mV (B), and 180 mV (C). See text for details of the measurement. The total area is normalized to one at each voltage. Note how the relative areas of the TC and CT states depend on voltage.

fraction of time channels spend in each state were created by binning single-channel current data until the relative areas of the peaks of the histograms no longer changed (±10%). Representative histograms are shown in Fig. 6. Compare the areas of peaks corresponding to the CT and TC states (A_{CT} versus A_{TC}). At low voltages, these are approximately equal (Fig. 6 A). As the applied voltage becomes more positive at the channel entrance, the relative area of the CT state peak increases and that of the TC peak decreases (compare Fig. 6 C). These relative areas are tabu-

lated for a range of voltages in Table 2. It can be seen from the table that the fraction of time the channel spends in the CC state also increases, and the time spent in the TT state decreases. The fraction of time a channel spends with a carbamate in the *cis* conformation at the entrance is given by the sum of areas of the CC and CT states ($A_{CC} + A_{CT}$) for positive voltages, and by the sum of the CC and TC states ($A_{CC} + A_{TC}$) for negative voltages. Fig. 7 A shows clearly that this fraction increases as the applied potential becomes more positive at the channel entrance.

The probability of finding both arms in the *cis* conformation (A_{CC}) is just the product of the probabilities of a *cis* at the entrance and a *cis* at the exit (($A_{CC} + A_{CT}) \times (A_{CC} + A_{TC})$) at all voltages (Table 2). This observation indicates

TABLE 2 Relative fractions of time spent in each conducting state as a function of voltage

| Applied voltage	A_{TT}	A_{TC}	A_{CT}	A_{CC}	$A_{(CC+CT)}$	$A_{(CC+CT)} \times A_{(CC+TC)}$
180	0.518	0.129	0.276	0.079	0.354	0.073
140	0.521	0.148	0.252	0.079	0.331	0.075
100	0.514	0.168	0.243	0.075	0.318	0.077
75	0.55	0.174	0.218	0.059	0.276	0.064
50	0.59	0.179	0.19	0.055	0.245	0.057
25	0.592	0.184	0.177	0.057	0.234	0.056

Gramicidin-EDA, 0.1 N HCl.

that the two arms isomerize independently. That is, the stability of a *cis* conformation at the channel entrance does not appear to depend on the conformation of the arm at the channel exit.

Voltage-independent behavior of gram-DMEDA

Gramicidin-DMEDA channels have the same structure as gram-EDA channels, except that the terminal amino groups of the arms carry two extra methyl groups in the DMEDA compound (Fig. 2). Electrostatically, these channels are very similar; it is primarily the steric bulk at the terminal position of the arm that distinguishes them.

Fig. 8 shows representative single-channel recordings of gram-DMEDA channels and the corresponding single-channel *I-V* plot. It is evident from the figure that the conductance properties of gram-DMEDA are qualitatively different from those of gram-EDA. There are only three conductance states, whereas gram-EDA shows four. In addition, the current magnitudes are greater than with gram-EDA, closer to those of unmodified gramicidin. Because we still expect four conformational states with approximately the same relative lifetimes as with gram-EDA, the observation of only three conductance states implies that two of the conformational states have the same conductance. The most likely possibilities are either that the conductance of the TC state is indistinguishable from that of the TT state or that the CT and TC states are indistinguishable. If we assume that the conformational behavior of the arms is independent (as seemed to be the case for gram-EDA), then an examination of the relative times spent in the three observed states can help us to distinguish these two possibilities.

Fig. 9 shows all-point histograms of time spent in states for gram-DMEDA in 0.1 M HCl at three different voltages. The areas of these histograms are plotted versus voltage in Fig. 7 *B*. At each voltage the ratio of areas of the peaks is ~70:26:4 (Fig. 7 *B*). If we assume that the middle peak is a superposition of the CT and TC states (A_{TC+CT}), then the CT and TC states individually would have a relative area of close to 0.13, because it is hard to imagine that one state would be much more stable than the other. Assuming independence of the arms, the relative area corresponding to the CC state is given by the probability of a *cis* at the entrance (($A_{TC+CT})/2 + A_{CC}$) times the probability of a *cis* at the exit
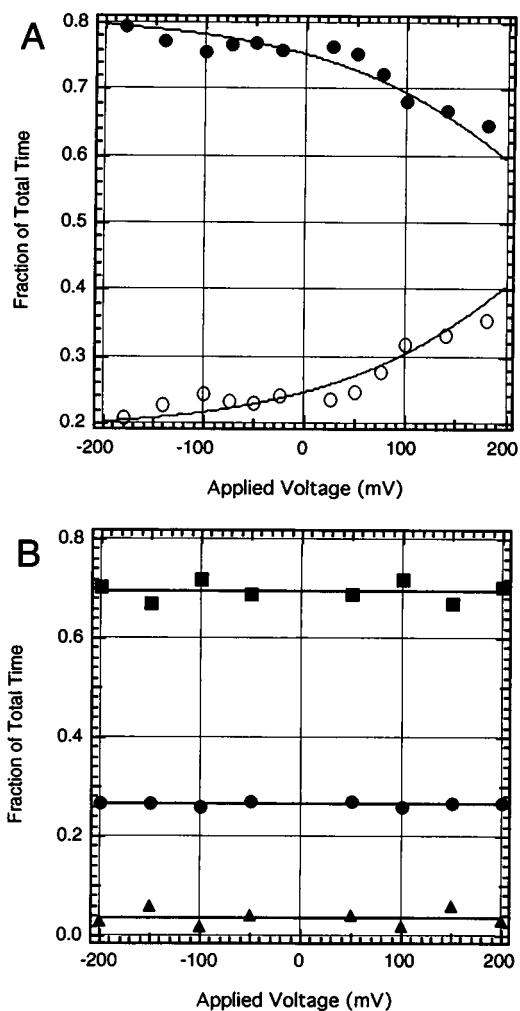
FIGURE 7 (*A*) Fraction of time spent by gram-EDA with a *cis*-carbamate (○) or a *trans*-carbamate (●) at the entrance, as a function of voltage. The fraction of time with a *trans*-carbamate is simply 1 − (fraction of time *cis*). The times correspond to the values for $A_{(CC+CT)}$ and $A_{(TC+TT)}$, respectively (see Table 2). Fitted curves are calculated by using Eq. 5 in the text. (*B*) Fraction of time spent by gram-DMEDA channels in each conducting state as a function of voltage (Table 3). ■, TT state; ●, TC and CT states; ▲, CC state.

(also ($A_{TC+CT})/2 + A_{CC}$). Calculated values for these relative areas are given in Table 3. At all three voltages this assumption leads to a reasonable correspondence between predicted and observed values for A_{CC}. Making the alternative assumption, that the middle peak corresponds to the CT state only, and TC and TT states are superimposed, predicts a value for A_{CC} larger than observed. Thus it appears both CT and TC states of gram-DMEDA give rise to the middle conductance state (as labeled in Fig. 9). Recall that similar behavior is observed for gram-EDA in the absence of an applied potential (Fig. 5 *C*); in that case, too, the CT and TC states have indistinguishable conductances.

It is evident from Fig. 7 *B* that voltage does not affect the relative time gram-DMEDA spends in the different conformational states. This is in direct contrast to the behavior of gram-EDA.

A

5 pA

500 ms

B

A

+50 mV at entrance

CC

CT + TC

TT

B

+100 mV at entrance

CC

CT + TC

TT

C

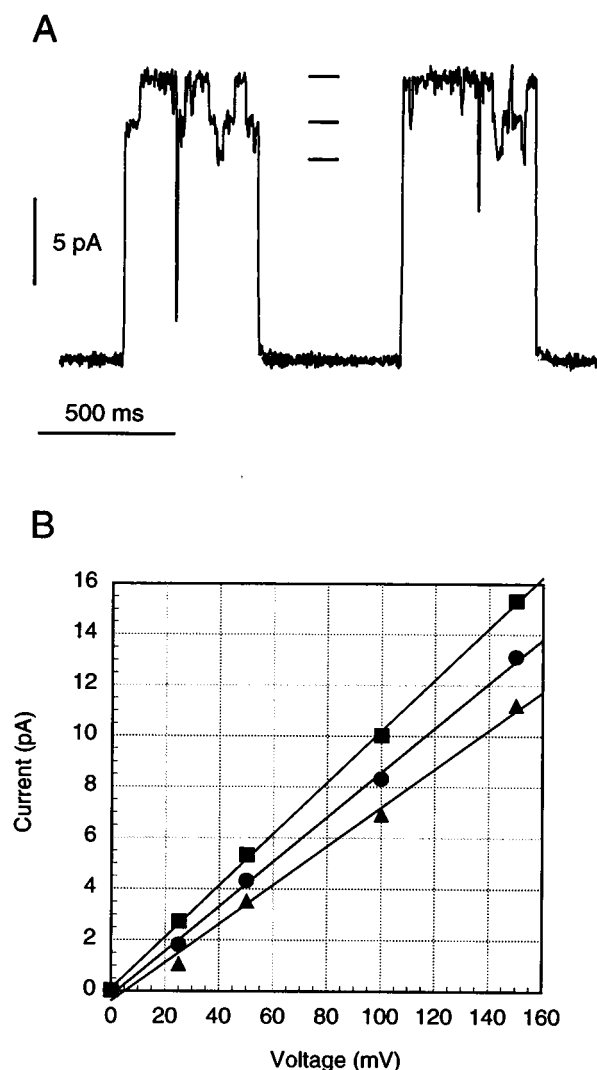+150 mV at entrance

CC

CT + TC

TT

FIGURE 8 (A) Single-channel currents of gram-DMEDA. Channels open upward from the baseline, and three conductance states are identified (indicated by the *bars*). The larger spikes are associated with flicker blocks, which are often observed with native gramicidin channels (Heinemann and Sigworth, 1990). (B) Single-channel current-voltage relationships for gram-DMEDA. Each state has a nearly linear *I-V* relationship. Conductances: ■, TT state, 100 pS; ●, TC and CT states, 86 pS; ▲, CC state, 70 pS.
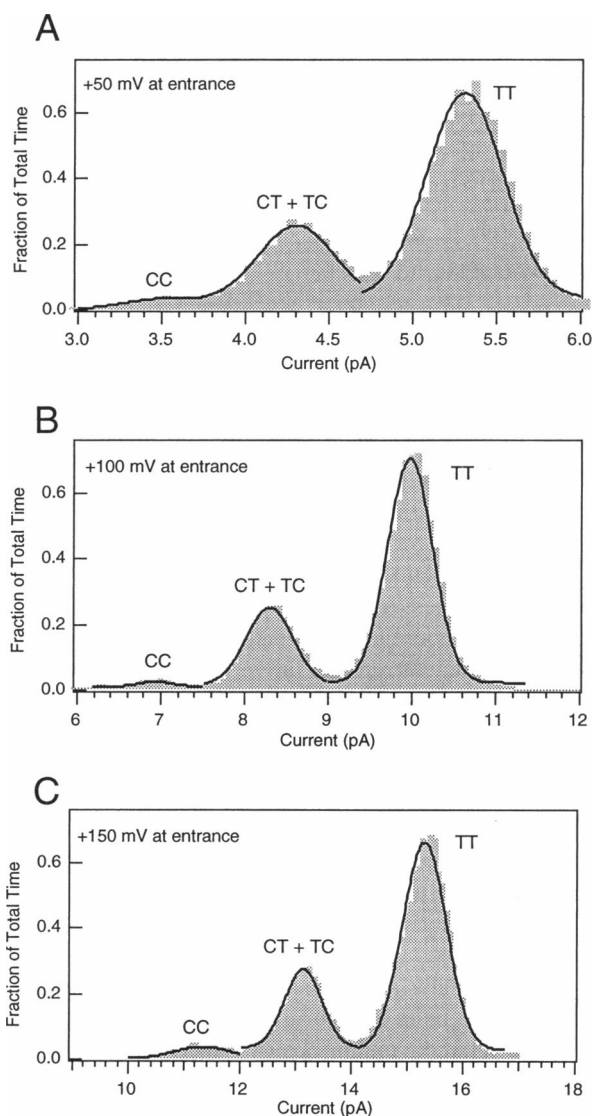
FIGURE 9 All-point histograms of time spent by gram-DMEDA in each conducting state at 50 mV (A), 100 mV (B), and 150 mV (C). See text for details of the measurement. The total area is normalized to one at each voltage.

The current-voltage relationship for each conductance state of gram-DMEDA is nearly linear (Fig. 8 B). This again is in direct contrast to the observed behavior of gram-EDA, and implies that the voltage-dependent conductance seen with gram-EDA reflects the voltage-dependent conformational behavior of the arm.

DISCUSSION

A model for the voltage dependence of the carbamate conformations

How does the applied voltage alter the *cis-trans* carbamate ratio of gram-EDA? It has been argued that the voltage does

not drop appreciably until quite close to or in the pore of the gramicidin channel (Jordan et al., 1989). Thus conformations of the arm that place the terminal ammonium group close to, or actually in, the pore mouth are likely to be most affected by voltage. Note that a positive potential at the channel entrance will promote movement of the tethered ammonium group into the channel, rather than out of it. We suggest that rotations of single bonds allow the arm to adopt conformations in which the ammonium group binds directly to the pore. *Cis-trans* ratios are affected because the arm can adopt conformations with a *cis*-carbamate that bind better (and are better stabilized by voltage) than those conformations possible with a *trans*-carbamate.

The most straightforward explanation for the lack of a voltage-dependence with gram-DMEDA is that the bulkier

TABLE 3   Relative fractions of time spent in each conducting state as a function of voltage

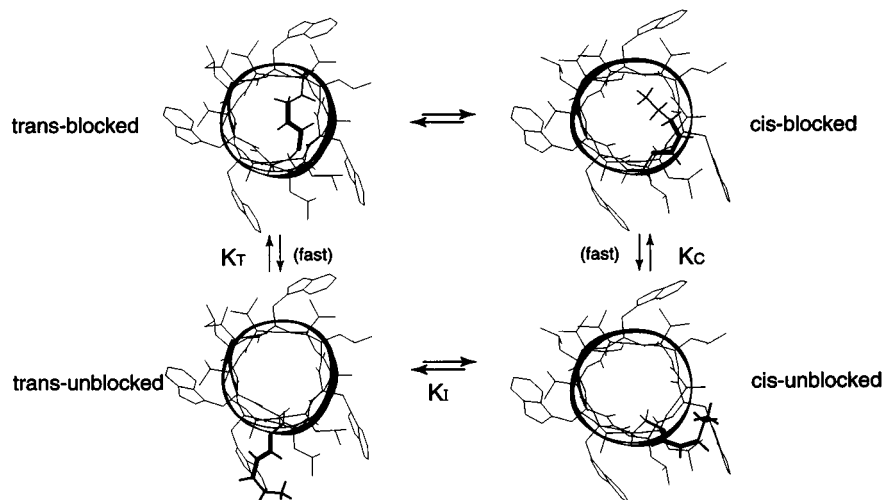| Applied voltage	A_{TT}	$A_{(TC+CT)}$	A_{CC}	$A_{(TC+CT)}/2 + A_{CC}$	$(A_{(TC+CT)}/2 + A_{CC})^2$
200	0.705	0.265	0.03	0.163	0.027
150	0.672	0.268	0.06	0.194	0.04
100	0.72	0.26	0.02	0.15	0.02
50	0.69	0.271	0.04	0.176	0.03

Gramicidin-DMEDA, 0.1 N HCl.

arm of gram-DMEDA cannot penetrate the mouth of the pore to any significant extent, so that the amino group senses none of the applied voltage. Cis-trans isomerization still causes a change in the average location of the charged amino group, and this affects ion flux electrostatically, but there is no effect of voltage on the location of this charge.

Consider one end of the gram-EDA channel only; we define four states: trans-blocked, trans-unblocked, cis-blocked, and cis-unblocked. Each of these is, in fact, an ensemble of states, representative members of which are diagrammed in Fig. 10. Cis and trans states are distinguished by the isomerization state of the carbamate bond in the arm. Bound and unbound states are distinguished by having a very low or zero conductance and a significant finite conductance, respectively. Because transitions to blocked states are not evident in the single-channel recordings, they are assumed to occur too rapidly to be detected directly. Transitions between cis and trans states are evident in the recordings.

These four states are connected as shown in Fig. 10 and are assumed to be in equilibrium. The cis-unblocked/trans-unblocked interconversion occurs outside the voltage gradient and is assumed to be voltage independent. The corresponding equilibrium constant can be written

$$K_I = \exp\left[\frac{-\Delta G_I}{RT}\right] = \frac{[trans\text{-unblocked}]}{[cis\text{-unblocked}]} \quad (1)$$

where $\Delta G_I = G_{trans(unblocked)} - G_{cis(unblocked)}$ (i.e., the free energy of trans-cis isomerization), R is the gas constant, and T is the absolute temperature.

The equilibria between blocked and unblocked states of gram-EDA are voltage dependent. For equilibria occurring at the channel entrance (which we assume are independent of those occurring at the channel exit), we can write

for trans:

$$K_{Tn}(\psi) = \exp\left[\frac{(-\Delta G_{To} + (k_T F \psi))}{RT}\right] = \frac{[trans\text{-blocked}]}{[trans\text{-unblocked}]} \quad (2)$$

for cis:

$$K_{Cn}(\psi) = \exp\left[\frac{(-\Delta G_{Co} + (k_C F \psi))}{RT}\right] = \frac{[cis\text{-blocked}]}{[cis\text{-unblocked}]} \quad (3)$$

where the subscripts Tn, Cn denote trans-entrance and cis-entrance respectively, ψ is the applied voltage (positive for a positive voltage at the channel entrance), F is the Faraday constant, and k_T and k_C and are constants that depend on the fraction of the applied field sensed by the arm for the trans and cis states, respectively. ΔG_{To} and ΔG_{TCo} are the free energies of binding of the arm to the pore in the absence of a voltage for the trans and cis states, respectively. The fraction of time a channel has a cis carbamate at the entrance is given by

$$f(cis)(\psi) = \frac{[cis\text{-blocked}] + [cis\text{-unblocked}]}{\begin{array}{l}[cis\text{-blocked}] + [cis\text{-unblocked}] \\ + [trans\text{-blocked}] + [trans\text{-unblocked}]\end{array}} \quad (4)$$

$$f(cis)(\psi) = \left(\frac{1 + K_{Cn}(\psi)}{1 + K_{Cn}(\psi) + K_I + (K_I K_{Tn}(\psi))}\right) \quad (5)$$

This expression contains five parameters: ΔG_I, ΔG_{To}, ΔG_{Co}, k_T and k_C. Some limits can be put on their values,

FIGURE 10   Model of voltage-dependent blocking of gram-EDA by the tethered gate. The diagram shows the an end-on view of the channel (only one monomer is shown). Four states are identified: cis and trans states are distinguished by the conformation of the carbamate bond in the gate (bold lines). These interconvert slowly (the activation barrier is 60 kJ/mol; Jaikaran and Woolley, 1995). Rotations of single bonds in the arms can result in conformations that block the channel. These states are assumed to interconvert quickly, i.e., faster than can be resolved by the single-channel recording apparatus. The extent to which the gate actually enters the pore mouth is unknown. Conformations shown are for illustrative purposes only.

trans-blocked

cis-blocked

K_T (fast)

(fast) K_C

trans-unblocked

K_I

cis-unblocked

TABLE 4 Values for the constants in the model presented (Eqs. 5, 8–11)

Variable	Value
ΔG_{To}	7.5 kJ/mol
ΔG_{Co}	2.2 kJ/mol
k_T	0
k_C	0.2
C_{TTo}	100 pS
C_{CTo}	86 pS
C_{TCo}	86 pS
C_{CCo}	70 pS
ΔG_I	−3.5 kJ/mol

Parameters obtained by fitting to the experimental data in Figs. 4 A and 7 A are given in italics. The errors in these values are interdependent but are estimated to be on the order of 30%. Conductances for the unblocked states of the channel are taken from the gram-DMEDA data (Fig. 8) and are not fitted parameters. The value for ΔG_I is also not a fitted parameter and comes from the cis-trans ratios of gram-DMEDA, i.e., -RT([trans]/[cis]).

however: k_T and k_C must be numbers between 0 and 1; ΔG_I is a measure of the intrinsic cis-trans ratio of the carbamate bond and can be estimated to be −3.5 kJ/mol from the cis-trans ratios observed with gram-DMEDA, if we assume the arms do not interact with the pore in that case (Fig. 7 B). The model and Eqs. 2 and 3 also lead to predictions about the voltage-dependence of channel conductance, because the extent of blocking affects the measured conductance. The experimental conductance data, along with the data for the voltage dependence of cis-trans ratios, can thus be used to define values for ΔG_{To}, ΔG_{Co}, k_T, and k_C (vide infra).

A model for the voltage-dependent conductance behavior of gram-EDA

To extend the model presented in Fig. 10 to permit a description of the effects of voltage on channel conductance, we need to consider the arms at both ends of the channel. By exact analogy with Eqs. 2 and 3, which described voltage-dependent blocking at the channel entrance, expressions for the process at the channel exit can be written as

$$K_{Tx}(\psi) = \exp\left[\frac{(-\Delta G_{To} - (k_T F\psi))}{RT}\right] \quad (6)$$

$$K_{Cx}(\psi) = \exp\left[\frac{(-\Delta G_{Co} - (k_C F\psi))}{RT}\right] \quad (7)$$

If we make the simplifying assumption that blocked states have zero conductance, then the conductance of each of the states of gram-EDA is given by

$$C_{CC}(\psi) = C_{CCo}\left(\frac{1}{1 + K_{Cn}(\psi)}\right)\left(\frac{1}{1 + K_{Cx}(\psi)}\right) \quad (8)$$

$$C_{CT}(\psi) = C_{CTo}\left(\frac{1}{1 + K_{Cn}(\psi)}\right)\left(\frac{1}{1 + K_{Tx}(\psi)}\right) \quad (9)$$

$$C_{TC}(\psi) = C_{TCo}\left(\frac{1}{1 + K_{Tn}(\psi)}\right)\left(\frac{1}{1 + K_{Cx}(\psi)}\right) \quad (10)$$

$$C_{TT}(\psi) = C_{TTo}\left(\frac{1}{1 + K_{Tn}(\psi)}\right)\left(\frac{1}{1 + K_{Tx}(\psi)}\right) \quad (11)$$

where C_{TTo} refers to the conductance of the unblocked TT state, $C_{TT}(\psi)$ to the observed conductance of the TT state (which is a function of the applied voltage), and likewise for C_{TC}, C_{CT}, and C_{CC}. Values for the conductances of the unblocked states can be taken from the corresponding values for the conductance of gram-DMEDA states. This gives C_{TTo} = 100 pS, C_{CTo} = C_{TCo} = 86 pS, and C_{CCo} = 70 pS (Fig. 8). The other parameters in these equations are the same ones used to describe the voltage dependence of the cis-trans carbamate ratios, i.e. ΔG_{To}, ΔG_{Co}, k_T and k_C. Simultaneous fitting of both sets of experimental data can provide estimates for the values of these parameters. Optimized values are collected in Table 4. The curves predicted by these equations, using the parameters in Table 4, are drawn as smooth lines fitted to the experimental data points in Figs. 4 A and 7 A.

Critique of the model

The model provides a reasonable description of both the voltage dependence of the conformation (cis-trans ratios) and the voltage dependence of the conductance for gram-EDA, because the calculated curves fit the experimental data quite well (Figs. 4 A and 7 A). Nevertheless, several assumptions in the analysis may be questioned, for instance: 1) The values for unblocked conductance are assumed to be equal to the corresponding values for gram-DMEDA and are assumed voltage independent. If the value for C_{TTo} is too low, for example, then k_T would not be zero, i.e., there could be a voltage-dependent interaction of the arm with the pore, even when the carbamate is in the trans conformation. In addition, the I-V curve of the unblocked TT state may be intrinsically nonlinear. 2) There is uncertainty in the statement that the movement of the two arms is independent, because the accuracy of the cis-trans ratio data is not high. If the relative stability of a state does depend on the conformational state at the other end of the channel, then more complex voltage-dependent behavior may be expected. 3) If the "blocked" state is not actually blocked but just of low conductance, then again, expressions for the voltage dependence of the conductance would be considerably more complex. Such expressions may, however, provide a better fit to the data.

It is conceivable that the arms alter the conductance electrostatically or sterically without actually entering and blocking the channel (as is proposed for the gram-DMEDA analog). Although this possibility cannot be ruled out, it would perhaps be surprising, if it were the case, to then find the same relative conductance changes upon isomerization independent of ion type (Fig. 1). For instance, H^+ and Cs^+ ions move through solution in different ways (Pomes and

Roux, 1996, 1997; Roux and Karplus, 1994). Whereas a complete blockage of the channel would affect both ions equally, a reconfiguration of the steric and electrostatic environment at the channel entrance may not. In the case of gram-DMEDA, where blockage does not appear to occur, the conductance of the CT and TC states is the same in 0.1 M HCl. This indicates that a *cis* arm at the channel entrance and at the exit has the same effect of H^+ conductance. The same is not true of Cs^+ conductance; in that case isomerization at the entrance has a more pronounced effect on conductance (data not shown; Woolley et al., 1995). More conclusive evidence for or against complete blockage might be obtained from single-channel current noise analysis (Heinemann and Sigworth, 1988, 1990).

Structural interpretations

The voltage dependence of gram-EDA is not strong. Although there is considerable uncertainty in the estimates of k_C and k_T derived from the fitting (Table 4), it appears that only 20% of the applied field is sensed by the *cis* arm—a considerably weaker voltage dependence than that found when hexafluorovaline was substituted at position 1 of hybrid gramicidin channels (Oiki et al., 1995). The value of 20% is similar to that derived with the three-barrier, two-site model to fit current-voltage data for the permeation of methylammonium ions (and other cations) through gramicidin channels (Seoh and Busath, 1993). Although this may reflect interaction of the ammonium group on the arm with an ion-binding site located 8–9 Å from the center of the channel (Busath, 1993), independent evidence (e.g., from NMR measurements) would be needed to substantiate this.

NMR spectroscopy has been used to measure the interaction of NH_4^+ with gramicidin incorporated into lysophosphatidylcholine membranes (Hinton et al., 1988). A dissociation constant of ~ 12 mM can be derived from those data. Analysis of conductance data gives a value of >100 mM for the dissociation constant of methylammonium. Ethylammonium is negligibly permeant (Eisenman et al., 1977; Hemsley and Busath, 1991; Seoh and Busath, 1993), and it does not inhibit K^+ flux, at concentrations up to 100 mM (Hemsley and Busath, 1991). The structure of the gate in the present case is similar to that of an ethylammonium ion with a carbamate group attached. If it were not tethered, such a group would be expected to have a very weak affinity for the pore. Attachment of the arm to the C-terminal end of gramicidin makes binding of the ammonium group in gram-EDA an intramolecular process, significantly increasing the effective molarity of the group (Kirby, 1980). The off rate for the blocking group could still be large, however, consistent with the notion that blocks occur significantly faster than the time resolution of the single-channel recording apparatus. A comparison of the equilibrium constants derived from the fitting (K_{To} and K_{Co}, corresponding to ΔG_{To} and ΔG_{Co}) indicates that the effective molarity for the tethered ammonium group is ~ 10-fold greater for the *cis*

conformer than for the *trans* conformer (in the absence of an applied voltage). This finding highlights the effect that a small geometrical reorganization can have on reaction rates (Kirby, 1980).

SUMMARY

The behavior of the gram-EDA derivative is consistent with a "ball-and-chain" model in which a voltage of the correct sign can promote binding of the C-terminal, positively charged arm to the pore and thereby block channel current. Blocking is most effective with a *cis*-carbamate conformation of the arm. In terms of engineering channel gating, more effective blocking groups might be obtained with more polar arms that exhibit higher effective molarities for binding to the pore. Alternatively, more rigid derivatives might permit control of gating via steric and electrostatic effects if groups could be positioned directly over the channel mouths.

REFERENCES

Andersen, O. S. 1983. Ion movement through gramicidin A channels. Single-channel measurements at very high potentials. *Biophys. J.* 41: 119–133.

Apell, H. J., E. Bamberg, H. Alpes, and P. Lauger. 1977. Formation of ion channels by a negatively charged analog of gramicidin A. *J. Membr. Biol.* 31:171–188.

Apell, H. J., E. Bamberg, and P. Lauger. 1979. Effects of surface charge on the conductance of the gramicidin channel. *Biochim. Biophys. Acta.* 552:369–378.

Bamberg, E., H. J. Apell, H. Alpes, E. Gross, J. L. Morell, J. F. Harbaugh, K. Janko, and P. Lauger. 1978. Ion channels formed by chemical analogs of gramicidin A. *Fed. Proc.* 37:2633–2638.

Busath, D. 1993. The use of physical methods in determining gramicidin channel structure and function. *Annu. Rev. Physiol.* 55:473–501.

Busath, D., and G. Szabo. 1988. Low conductance gramicidin A channels are head-to-head dimers of $\beta^{6.3}$-helices. *Biophys. J.* 53:689–695.

Cifu, A. S., R. E. Koeppe, II, and O. S. Andersen. 1992. On the supramolecular structure of gramicidin channels. The elementary conducting unit is a dimer. *Biophys. J.* 61:189–203.

Eisenman, G., J. Sandblom, and E. Neher. 1977. Ionic selectivity, saturation, binding, and block in the gramicidin A channel: a preliminary report. *In* Metal-Ligand Interactions in Organic Chemistry and Biochemistry, Part Two. D. Reidel Publishing Company, Dordrecht, the Netherlands. 1–36.

Heinemann, S. H., and F. J. Sigworth. 1988. Open channel noise. IV. Estimation of rapid kinetics of formamide block in gramicidin A channels. *Biophys. J.* 54:757–764.

Heinemann, S. H., and F. J. Sigworth. 1990. Open channel noise. V. Fluctuating barriers to ion entry in gramicidin A channels. *Biophys. J.* 57:499–514.

Hemsley, G., and D. Busath. 1991. Small iminium ions block gramicidin channels in lipid bilayers. *Biophys. J.* 59:901–908.

Hille, B. 1992. Ionic Channels of Excitable Membranes. Sinauer Associates, Sunderland, MA.

Hinton, J. F., J. Q. Fernandez, D. C. Shungu, W. L. Whaley, R. E. Koeppe, II, and F. S. Millett. 1988. Tl-205 nuclear magnetic resonance determination of the thermodynamic parameters for the binding of monovalent cations to gramicidins A and C. *Biophys. J.* 54:527–533.

Jaikaran, D. C. J., and G. A. Woolley. 1995. Characterization of thermal isomerization at the single molecule level. *J. Phys. Chem.* 99: 13352–13355.

Jin, X. Z. 1992. The impact of the negative charge on cation permeation in the taurine[16]-gramicidin channel. Ph.D. thesis. Brown University, Providence, RI.

Jordan, P. C., R. J. Bacquet, J. A. McCammon, and P. Tran. 1989. How electrolyte shielding influences the electrical potential in transmembrane ion channels. *Biophys. J.* 55:1041–1052.

Ketchem, R. R., W. Hu, and T. A. Cross. 1993. High resolution structure of gramicidin in a lipid bilayer by solid-state NMR. *Science.* 261: 1457–1460.

Kirby, A. J. 1980. Effective molarities for intramolecular reactions. *Adv. Phys. Org. Chem.* 17:183–278.

Koeppe, R. E., II, and O. S. Andersen. 1996. Engineering the gramicidin channel. *Annu. Rev. Biophys. Biomol. Struct.* 25:231–258.

Lien, L., D. C. J. Jaikaran, Z. Zhang, and G. A. Woolley. 1996. Photomodulated blocking of gramicidin ion channels. *J. Am. Chem. Soc.* 118:12222–12223.

MacKinnon, R., R. Latorre, and C. Miller. 1989. Role of surface electrostatics in the operation of a high-conductance Ca^{2+}-activated K^+ channel. *Biochemistry.* 28:8092–8099.

Myers, V. B., and D. A. Haydon. 1972. Ion transfer across lipid membranes in the presence of gramicidin A. II. The ion selectivity. *Biochim. Biophys. Acta.* 274:313–322.

Oiki, S., R. E. Koeppe, II, and O. S. Andersen. 1995. Voltage-dependent gating of an asymmetric gramicidin channel. *Proc. Natl. Acad. Sci. USA.* 92:2121–2125.

Pomes, R., and B. Roux. 1996. Structure and dynamics of a proton wire: a theoretical study of H^+ translocation along the single-file water chain in the gramicidin A channel. *Biophys. J.* 71:19–39.

Pomes, R., and B. Roux. 1997. Free energy profiles governing H^+ conduction in proton wires. *Biophys. J.* 72:A246.

Reinhardt, R., K. Janko, and E. Bamberg. 1986. Single channel conductance changes of the desethanolamine-gramicidin through pH variations. *In* Electrical Double Layers in Biology. Plenum Press, New York. 91–102.

Roeske, R. W., T. P. Hrinyo-Pavlina, R. S. Pottorf, T. Bridal, X. Z. Jin, and D. Busath. 1989. Synthesis and channel properties of [Tau[16]]-gramicidin A. *Biochim. Biophys. Acta.* 982:223–227.

Roux, B., and M. Karplus. 1994. Molecular dynamics simulations of the gramicidin channel. *Annu. Rev. Biophys. Biomol. Struct.* 23:731–761.

Seoh, S. A., and D. Busath. 1993. The permeation properties of small organic cations in gramicidin A channels. *Biophys. J.* 64:1017–1028.

Stankovic, C. J., S. H. Heinemann, and S. L. Schreiber. 1991. Photomodulated ion channels based on covalently linked gramicidins. *Biochim. Biophys. Acta.* 1061:163–170.

Sukhanov, S. V., B. B. Ivanov, S. Y. Orekhov, L. I. Barsukov, and A. S. Arseniev. 1993. Molecular design of photo-modulated ion channels based on gramicidin A and their electrochemical properties (in Russian). *Biol. Membr.* 10:535–543.

Woolley, G. A., A. S. I. Jaikaran, Z. Zhang, and S. Peng. 1995. Design of regulated ion channels using measurements of *cis-trans* isomerization in single molecules. *J. Am. Chem. Soc.* 117:4448–4454.

Woolley, G. A., A. S. I. Jaikaran, Z. Zhang, and S. Peng. 1996. Voltage-dependence of a designed ion channel. *In* Peptides: Chemistry, Structure and Biology. Mayflower Scientific, Kingswinford, England. 601–602.